Numerical and Experimental Analysis of High-Stress Wire Connections in Offshore Fish Farming Cages for Site-specific Lifetime Prediction

J. Straub[a,b,1], A. Eckhardt[a] L. Bošković[a,b]

[a]WITg – Institute for Material Systems Technology Thurgau,
Konstanzerstrasse 19, CH-8274 Tägerwilen, Switzerland
[b]Materials Engineering Laboratory, HTWG Konstanz University of Applied Sciences,
Alfred-Wachtel-Str. 8, D-78462 Konstanz, Germany

Abstract

With climate change and the steady increase in the world's population, fish farming is becoming an increasingly important topic in terms of expanding a sustainable food supply. Such farms are primarily equipped with plastic meshes. A new approach is to replace conventional meshes with steel mesh, which has many advantages. However, the local environmental conditions put a lot of strain on the structures, resulting in repeated wire breakages. As part of the investigations presented in the search for a way to avoid such damage, detailed components of a cage are tested via simulation and laboratory tests. It turns out that many of the effects occurring in the field can be modelled with simple modelling. The combination of force, strain and displacement measurement makes it possible to draw conclusions from the main load scenarios of real applications.

Keywords

Stainless Steel, Computational Structural Mechanics, Fatigue, Numerical and experimental analysis of stainless steel wire connections

1 Introduction

Due to global change in terms of global warming, overfishing of natural fish populations and the rapid increase in the world's population, solutions must be found to feed a large proportion of the 10 billion people predicted to be living on the planet by 2060 [1] [2]. Chile took off in the 1980s with salmon and trout farming [3] and is now one of the main exporters of farmed fish. Many offshore fish farm sites are located in the fjords of the rugged coast of the Lagos and Aysén regions. The harsh conditions prevailing there lead to strong waves and directional currents, which place a heavy load on fish farms [4]. The standard cages built with nylon meshes are being replaced by our project partner with meshes made of high-strength stainless steel. This measure reduces expensive cleaning intervals, avoids water pollution from microplastics, protects the fish from predators thanks to its high strength and reduces the mixing of farmed and wild fish. Although the high material strength means that small wire diameters and therefore easier flow through the structure can be realised [5], the stresses there lead to wire breakage despite the advantages mentioned. This indicates that metallic, stiffer meshes behave differently to conventional plastic meshes [6] and must therefore also be investigated separately.

The map of scientific work on the subject of fish farms is extensive. Fish farms are often viewed from a somewhat more distanced perspective than is the case in our studies. In many cases, the centre of investigation is the mooring system with which the mesh of a farm is held in position. [7] shows that pretensioning this farm periphery leads to more failures and also attempts to determine fatigue damage by calculation [8]. The fact that large waves in particular can have a considerable influence on the loads on a cage is illustrated by [9]. [10] also shows that the wave height is directly related to the load on the structures and also confirms the increase in load on cages due to the growth of marine organisms. This fact is confirmed by studies carried

[1]Corresponding author.
E-mail address: j.straub@witg.ch
https://witg.ch/aktuell

out in parallel to these. Wire structures with a flow through them are also represented by porous media and their degree of fouling changes, which leads to load differences at a constant flow velocity. Although [11] postulates that cages made entirely of steel wire are very well suited for offshore fish farming due to their low reduction in shape and volume, high material strengths and rigid structures react sensitively to permanent and cyclical tensile loads.

The basic approach in the investigation is the continuous comparison of test and field data with numerical calculation results. The measured and result variables are deformations, forces and strains. In the first step, various project components (clamping devices of the laboratory tests, subsections One-Link (OL) and Multi-Link (ML) of a fish farm, reduced image of the entire fish farm) are virtually modelled and then calculated using FEA. The results from calculations are then compared with information from the field and from laboratory tests, which ultimately leads to a calibration/adjustment (adaptation) of the simulation models. It can therefore be said that this is an optimisation control loop in order to ultimately be able to make service life statements/improvement suggestions for increasing longevity by simulating very large fish farm constructions that can no longer be reproduced in the laboratory.

Firstly, the general procedure of the study is briefly described. The next step is an overview of the software and hardware used. This is followed by an explanation of how the numerical models are structured. Finally, all results are presented and critically discussed. A conclusion with an outlook concludes the paper.

2 Materials and Methods

As already mentioned, the methodology used in the study is an iterative procedure that is divided into the areas of FEA and laboratory testing and thus includes numerical modelling, experimental test setup and execution as well as the comparison of virtual and practical results. Finite element models (FEM) are created for the simulations, considering the relevant boundary conditions and material properties. An experimental test setup is then carried out with boundary conditions identical to the simulations. The results from the tests are then compared with the simulation models and optimised at the same time (boundary conditions, material data). If a measurement method does not work, a solution is sought with which the desired results can be generated.

2.1 Software and Hardware

Solid Works 2024 was used to create the CAD data. Final adjustments to the models in preparation for calculations were always carried out using Ansys Space Claim 2023 R2. All calculations were carried out using static mechanical analysis systems in Ansys Workbench 2023 R2. A servo-hydraulic universal testing machine (LFV100) was used to carry out the tests. With this machine, test forces of ±100 kN and test frequencies of up to 50 Hz can be realised.

The main object of the tests is the smallest unit of a fish farm cage, known as a one-link (OL), a mesh section consisting of 3x5 OLs called a multi-link (ML) and a clamping device for ML. The wires for the links are made of duplex steel 1.4462 and are available in diameters of 2 and 3 mm. An overview of the average results from tensile tests of the links is shown in Table 1. For quasi-static and cyclic tests, clamping fixtures developed in-house are used, which represent the actual boundary conditions as closely as possible (Figure 1).

The DEWE-43-A 8-channel data acquisition box with quarter-bridge extension plug was used to analyse strain gauges applied to specimens and fixtures. The strain gauges are uniaxial foil strain gauges with a nominal resistance of 120 ohms and a measuring grid size of 0.65x1.0 mm (Figure 2 a.) and 2.0x1.2 mm (Figure 2 b.), which were applied using a cyanoacrylate single-component adhesive.

Table 1. Results of tensile tests of One- and Multi-Links.

Specimen	Parameter	Value
Straight wire 2mm	Yield strength	1467 MPa
	Tensile strength	1712 MPa
One-Link 2 mm	Breaking force	5,4 kN
One-Link 3 mm		12,1 kN
Multi-Link 2 mm		24,2 kN

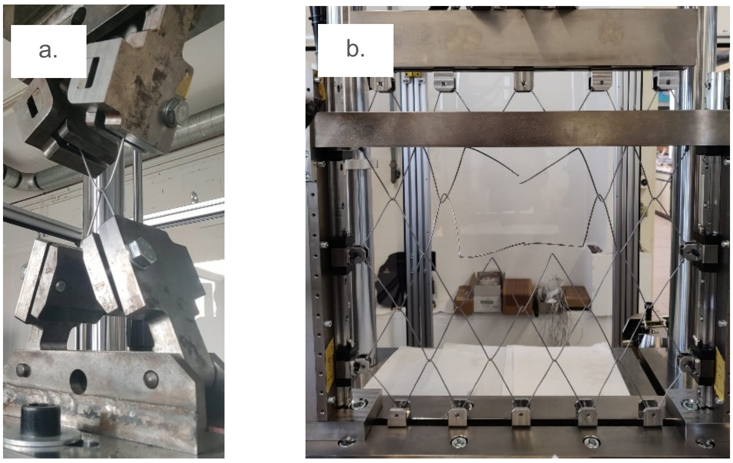

Figure 1.a. Clamping device of a One-Link, b. Clamping Device of a Multi-Link.

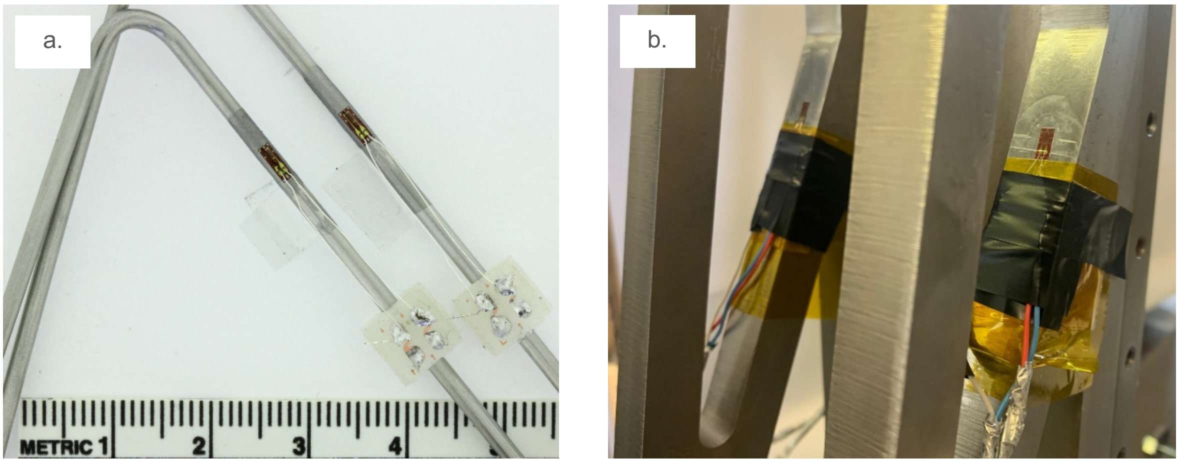

Figure 2. Applied strain gauges: a. One-Link, b. Clamping Device of a Multi-Link.

2.2 Simulation Setup

In this study, several numerical volume models are set up in linear and non-linear structural-mechanical analysis systems. The background to this is that it reduces the complexity of the individual models on the one hand and on the other hand opens up the possibility of illuminating the centre of the investigation from several angles.

The boundary conditions are set based on the connection of the cage components in a real fish farm. This means that an OL is relatively firmly clamped and an ML has slightly more open degrees of freedom. This is illustrated in the schematic replacement models of the OL and ML test set-up in Figure 3.

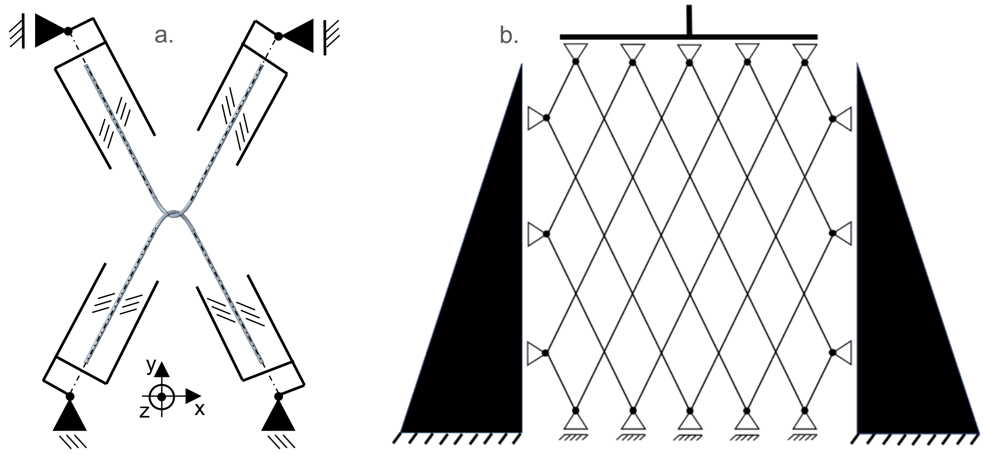

Figure 3.a. Schematic structure of an OL-clamping device,
b. Schematic structure of a ML-clamping device.

The load conditions are derived from the two main environmental conditions that cause damage, the waves and the current. These primarily lead to tensile loads, as the wire mesh would compress under pressure and would not be loaded. Due to the dead load of the cage as well as the permanent current and water movement, it can be assumed that a tensile swell load is involved in a cyclic analysis.

The models made of 2 mm and 3 mm wire are manufactured using different production processes and therefore differ mainly in the shape of the wire legs. For the sake of simplicity, a 2 mm wire and straight wire legs are always used for the simulations. It is known from earlier investigations [12] that the agreement between calculation and test results is very good despite the simplification of the shape.

The tensioning device for ML is planned, calculated and built as part of the investigations so that quasi-static and cyclic tests can then be carried out. The calculation model for the fixture is set up in two analysis systems. A distinction is made between the static base frame (attached to the T-slot plate of the LFV100) and the movable crosshead (attached to the hydraulic piston) (Figure 4).

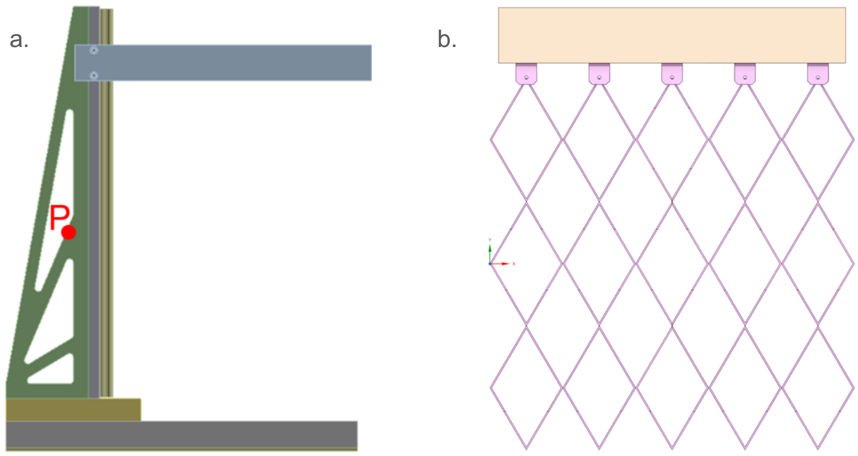

Figure 4.a. Model of the ML-clamping device, b. Model of the traverse with the ML.

The base frame is calculated in half, whereby the crossbeam is completely simulated with 3x5 ML. For the sake of simplicity, the ML lies in the xy-plane and consists of simplified rhomboids that are connected to the ML with universal joints at their tips. The effects that are neglected can be modelled in detail using OL or even smaller submodels [12]. Screw connections (M5, M6, M8, M16) are modelled as a line to which a corresponding diameter is assigned. It is fixed via contact condition ‘fixed connection’ in the hole base and in the counterbore for the cylindrical bolt head and preloaded by bolt preload force according to [13] in the first analysis load step.

The meshing strategy initially follows the trial-and-error principle for all simulation models in order to be able to retrieve initial results. The areas identified as critical to failure are then successively refined and the stress results are ultimately validated by means of a network convergence study. In contact areas, finer meshing is carried out directly for reliable contact target determination. All simulation models mainly consist of the SOLID187 and SOLID186 [14] elements for the volumes, CONTA174 and TARGE170 elements for contact areas and BEAM188, MPC184 and PRETS179 for the screw connections.

All models are designed differently. When considering the OL, the calculation is always non-linear. This means that both the frictional wire contact area, large deformations and the bilinear isotropic hardening model lead to non-linearity. Parameter studies revealed only minor influences on the results by changing the coefficient of friction, so that this was set to $\mu = 0.2$.

The ML and the clamping device for it are calculated as linear-elastic. The background to this is safety against damage during the test, which is why it is assumed that the material used is below its yield point.

A comparison of all available contact algorithms showed that the penalty method delivers comparable results in a short time. Asymmetric contacts are recognised at Gaussian integration points and their stiffness is updated in each calculation iteration.

The direct solver is used for small models (<150,000 elements). If the number of elements exceeds 150,000, the iterative solver is used. A suitable time step is set depending on the model through several calculation runs. It is also important to ensure that the division of the results is fine enough. In concrete terms, this means that for OL models with 5 load steps and 5-20 substeps, a displacement of 5 mm is applied. With the ML tensioning device, for example, two load steps are sufficient, whereby the bolts are pretensioned in the first step and a displacement of around 3 mm is then introduced into the system over 30 sub-steps in the second step in order to generate the expected breaking force.

The credibility of the simulation results is verified by tensile tests, strain gauge measurements on the OL and ML wires and the ML tensioning device as well as deformation measurements of the ML tensioning device under load.

3 Results and Discussion

The simulation model of the OL with bilinear isotropic hardening model can reproduce the plastic deformation effects in the wire contact area (Figure 5) quite well. A notch is formed where the material begins to flow and eventually one side of the two half-meshes of an OL always breaks.

a. b.

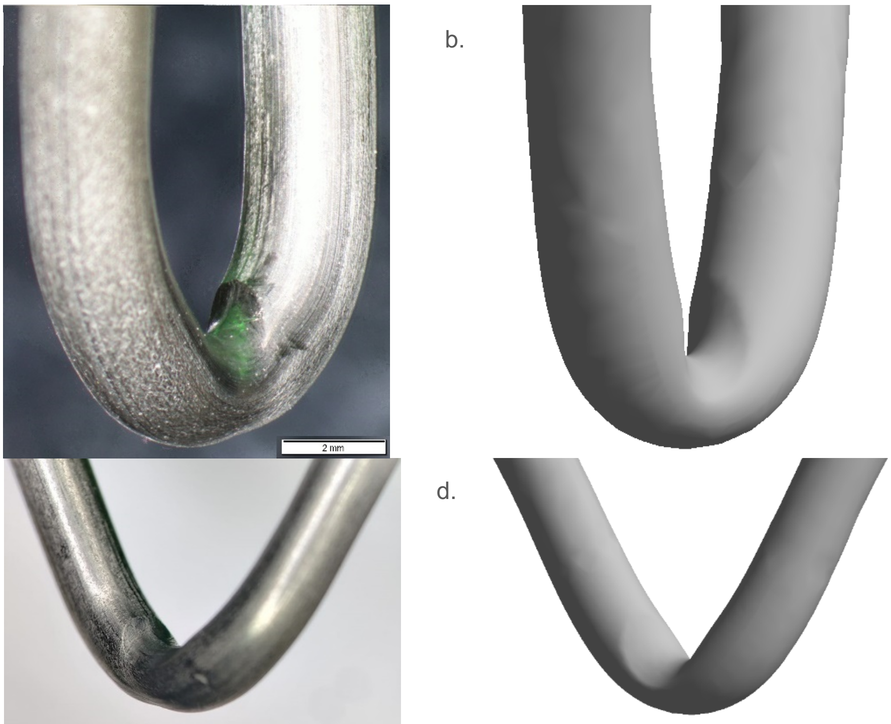

c. d.

Figure 5.a. Side view of the plastic deformations in the upper wires contact area of an OL-specimen shortly before it is broken, b. Side view of the simulation model of an OL after the applied load, c. Front view of the described specimen, d. side view of the described simulation model.

However, the force-displacement diagram from the averaged tensile tests does not fully match the simulation results (Figure 6). OL 1. gen. Is slightly less stiff than OL 2. gen. This was achieved by adjusting the tangent modulus (E_T). In the first simulation, this was one tenth of the yield strength and was then increased to E_T = 1000 MPa in the second simulation. This means that at least the breaking force of around 5.4 kN can be achieved. This result is classified as sufficiently accurate, as the failure patterns from the field are generally fatigue fractures that occur at much lower loads. The tests on the cyclically loaded OL and ML have not yet been finalised, which is why interim results are not presented. However, it can be said that both OL and ML fail at different points depending on the load horizon. It should be mentioned that no absolute numerical values for stresses occurring are published, as the differences between calculation and test have not yet been conclusively clarified. The different slopes of the curves from virtual and real tensile tests are currently attributed to the discrepancies between the materials. It is quite possible that the strong anisotropy of the wires deviates strongly from the isotropic model used.

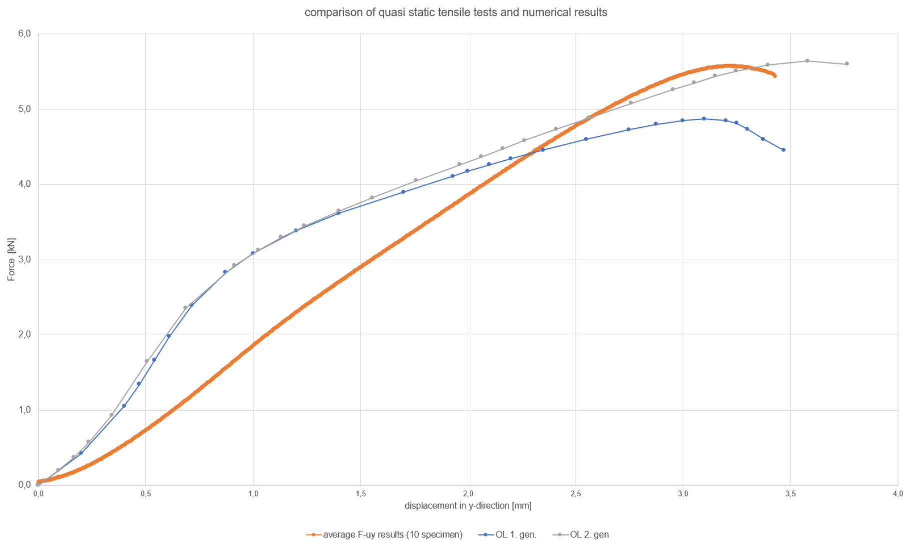

Figure 6. Comparison of quasi static tensile tests and numerical results of quasi static OL tests.

To validate the simulation results, various attempts were made to measure the strains directly on the wires. All attempts failed due to the filigree shape and geometric complexity of the wires. For this reason, the strain gauge applications were shifted from the wire directly to the ML clamping device (Figure 4 a. Marking P). A total of 4 strain gauges were applied and strains and associated loads were recorded as part of a quasi-static tensile test in order to compare them with the simulation results.

The measurement and simulation results are visualised in (Figure 7) In the diagram, the strain simulated or measured at point P is plotted as a function of the traverse force. Four strain gauge measurement curves and two simulation curves can be recognised. The reason for this is the symmetry of the simulation model of the ML clamping device.

Basically, it can be clearly seen for both measurement and simulation results that the strains follow a linear curve to the force applied to the traverse. While the simulation results are very similar to each other and are almost perfectly aligned, the strain gauge measurement curves are less similar to each other. The values of the measurement points of strain gauges 3 and 4 lie exactly on top of each other and are almost identical. However, strain gauges 1 and 2 show clear differences in their amounts. As strain gauges 1 and 2 are on the same side of the ML clamping device and their averaged values are approximately the same as those of strain gauges 3 and 4, the high discrepancy in the values of strain gauges 1 and 2 is due to a tolerance in the clamping device. It must also be mentioned at this point that the simulation models are always ideal conditions. The situation is different in reality, however, where the contact points of the ML to the clamping device are always slightly off-centre and this alone results in slight measurement differences.

If the simulation and strain gauge measurement results are compared with each other, it can be seen that the gradient of the curve of the simulation results is significantly higher than that of the strain gauge measurements. It is estimated that the amounts of the simulation results are therefore 50 % higher than those of the strain gauge measurement results. The increased strain amounts in the simulation indicate that the modelled ML generates significantly higher lateral forces in the simulation than the ‘real’ ML. This means that the boundary conditions in the simulation were designed to be too stiff. When looking at the ML clamping device, it is noticeable that there are some intermediate components that reduce the force flows and thus also the strains arriving at the strain gauges. In addition, bolt settlement effects were completely neglected.

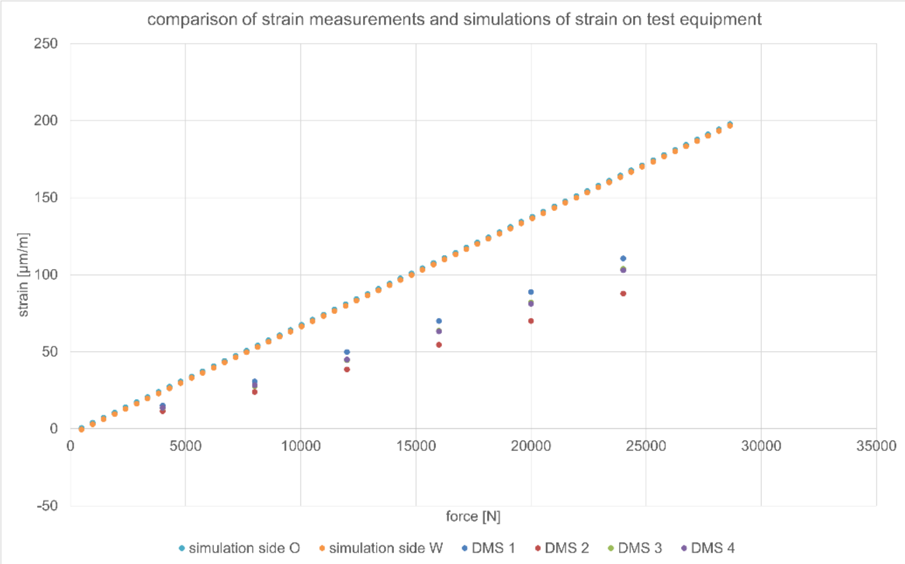

Figure 7. Comparison of strain measurements and simulations of strain on test equipment.

4 Conclusions

To summarise, it can be said that the approach pursued in the studies certainly has its justification. It attempts to pragmatically get to the core of the failure mechanisms. Virtual and practical tools are used to emphasise the credibility of results. The trial-and-error principle often encounters resistance that needs to be overcome. If results do not meet expectations, new approaches are sought. For example, strain gauge measurements on the smallest component of a fish farm became a somewhat more decentralised one. This allowed us to draw conclusions about the conditions in a network from the periphery of a network section. The reduced approach to any simulation models makes it possible to make quick changes and find new ways out of dead ends. This makes it possible to generate useful results for plastic deformations in the wire contact area of an OL using simple material models. This ensures general accessibility for our approaches.

Further investigations will mainly focus on refining the material model for OL simulations, as the agreement is not completely satisfactory. The ML models are also to be optimised. The correct modelling of the boundary conditions is particularly important here. One approach we are pursuing works with spring stiffness substitution models, which will make it possible to precisely adjust the stiffness of boundary conditions on the ML fixture. With regard to the effects of cyclic loading of OL and ML, tests are currently being carried out in which 1-2e+6 cycles are targeted. The results are used to generate component failure curves which can then be used to estimate the probability of survival. In combination with fluid-structure interaction models of complete fish farms, the circle can then be closed and finally stresses can be determined from total loads acting on fish farms in the field in sub-models of wire contacts.

5 Acknowledgement

The project was funded by Innosuisse (The Swiss Agency for Innovation Promotion). We thank the Geobrugg AG (CH) for the financial and organizational support of this research project. We would also like to thank the Institute for Materials Systems Technology - Thurgau, the Laboratory for Materials Systems Technology at the University of Applied Sciences and all employees who contributed their expertise to the project.

6 References

[1] Worldometer. World Population Projections. 14.02.2025 [Online]. Available: https://www.worldometers.info/world-population,

[2] FAO. 2024. "In Brief to The State of World Fisheries and Aquaculture 2024 - Blue Transformation in action", Rome, 2024, pp 9-10, https://doi.org/10.4060/cd0690en

[3] OECD, An Appraisal of the Chilean Fisheries Sector / Organisation for Economic Co-operation and Development, Paris: OECD Publishing, 2009, pp 21, ISBN 978-92-64-07395-1

[4] Buck B. H., Troell M. F., Krause G., Angel D. L., Grote B., Chopin T., „State of the Art and Challenges for Offshore Integrated Multi-Trophic Aquaculture (IMTA)“, Front. Mar. Sci., 15 May 2018, Volume 5, pp. 15-16, https://doi.org/10.3389/fmars.2018.00165

[5] Gümpel P., Hörtnagl A., Sorg M., „High Tensile Stainless Steel as a Sustainable Material for Aquaculture“, Procedia Manufacturing Volume 30, 2019, pp. 321, https://doi.org/10.1016/j.promfg.2019.02.045

[6] Cifuentes C., Tampier G., Echevarria A., Hurtado C. F., „Determination of Mooring Load Levels on a Cage Designed for Exposed Aquaculture in Chile“, Proceedings of the ASME 2023 42nd International Conference on Ocean, Offshore and Arctic Engineering. Volume 10: Professor Ian Young Honouring Symposium on Global Ocean Wind and Wave Climate; Blue Economy Symposium; Small Maritime Nations Symposium. Melbourne, Australia. June 11–16, 2023. V010T13A003. ASME, pp. 6-7, http://dx.doi.org/10.1115/OMAE2023-101308

[7] Hui-Min Hou, Guo-Hai Dong, Tiao-Jian Xu, Yun-Peng Zhao, Chun-Wei Bi, Fu-Kun Gui, „Fatigue reliability analysis of mooring system for fish cage“, Applied Ocean Research, Volume 71, 2018, pp. 88, https://doi.org/10.1016/j.apor.2017.12.008

[8] Hui-Min Hou, Guo-Hai Dong, Tiao-Jian Xu, „Fatigue damage distribution and reliability assessment of grid mooring system for fish cage“, Marine Structures, Volume 67, 2019, pp. 20, https://doi.org/10.1016/j.marstruc.2019.102640

[9] Zhongchi Liu, Haitong Xu, C. Guedes Soares, „Experimental study on the mooring forces and motions of a fish cage under regular waves“, Ocean Engineering, Volume 280, 2023, pp. 9-10, https://doi.org/10.1016/j.oceaneng.2023.114612

[10] Zhao, Zilong, Wenzhi Yu, and Tiaojian Xu. 2023. "Study of the Interaction between Regular Waves and a Wind-Fish Combined Structure" Applied Sciences 13, no. 5: 3103, pp. 14, https://doi.org/10.3390/app13053103

[11] Xiaoyu Qu, Fuxiang Hu, Taisei Kumazawa, Yohto Takeuchi, Shuchuang Dong, Daisuke Shiode, Tadashi Tokai, „Deformation and drag force of model square fish cages in a uniform flow“, Ocean Engineering, Volume 171, 2019, pp. 624, https://doi.org/10.1016/j.oceaneng.2018.12.016

[12] Straub J., Boškovic L., Bogatzky T., Dornbierer U, "Test based finite element analysis of wire meshes," Journal of Physics: Conference Series, Volume 2198, 15th Global Congress on Manufacturing and Management (GCMM 2021) 25th-27th November 2020, Liverpool, United Kingdom, pp. 3-7, doi: https://doi.org/10.1088/1742-6596/2198/1/012027.

[13] Fischer U., "Maschinenelemente: 5.2 Schrauben", in Tabellenbuch Metall, 44th ed., Haan-Gruiten, Deutschland, Europa-Lehrmittel, 2008, pp. 221

[14] Fiedler M., Wächter M., Varfolomeev I., Vormwald M., Esderts A., „Richtlinie Nichtlinear: Rechnerischer Festigkeitsnachweis unter expliziter Erfassung nichtlinearen Werkstoff-verformungsverhaltens: für Bauteile aus Stahl, Stahlguss und Aluminiumknetlegierungen“, Frankfurt am Main: VDMA Verlag GmbH, 2019, pp. 13-14, ISBN 978-3-8163-0729-7